Journal of Power Sources 196 (2011) 9107–9116

Contents lists available at ScienceDirect

Journal of Power Sources

journal homepage: www.elsevier.com/locate/jpowsour

Review

A review of polymer electrolyte membrane fuel cell durability test protocols

Xiao-Zi Yuan, Hui Li, Shengsheng Zhang, Jonathan Martin, Haijiang Wang*

Institute for Fuel Cell Innovation, National Research Council Canada, 4250 Wesbrook Mall, Vancouver, BC, Canada V6T 1W5

ARTICLE INFO

Article history:
Received 30 May 2011
Received in revised form 26 July 2011
Accepted 28 July 2011
Available online 23 August 2011

Keywords:
Accelerated test
Degradation
Diagnosis
Durability
PEM fuel cell
Protocol

ABSTRACT

Durability is one of the major barriers to polymer electrolyte membrane fuel cells (PEMFCs) being accepted as a commercially viable product. It is therefore important to understand their degradation phenomena and analyze degradation mechanisms from the component level to the cell and stack level so that novel component materials can be developed and novel designs for cells/stacks can be achieved to mitigate insufficient fuel cell durability. It is generally impractical and costly to operate a fuel cell under its normal conditions for several thousand hours, so accelerated test methods are preferred to facilitate rapid learning about key durability issues. Based on the US Department of Energy (DOE) and US Fuel Cell Council (USFCC) accelerated test protocols, as well as degradation tests performed by researchers and published in the literature, we review degradation test protocols at both component and cell/stack levels (driving cycles), aiming to gather the available information on accelerated test methods and degradation test protocols for PEMFCs, and thereby provide practitioners with a useful toolbox to study durability issues. These protocols help prevent the prolonged test periods and high costs associated with real lifetime tests, assess the performance and durability of PEMFC components, and ensure that the generated data can be compared.

Contents

1. Introduction

Owing to their high energy efficiency, convenient operation, and environmentally friendly characteristics, polymer electrolyte

---

* Corresponding author. Tel.: +1 604 221 3038; fax: +1 604 221 3001.
E-mail address: haijiang.wang@nrc.gc.ca (H. Wang).

0378-7753/$ – see front matter. Crown Copyright © 2011 Published by Elsevier B.V. All rights reserved.
doi:10.1016/j.jpowsour.2011.07.082

membrane fuel cells (PEMFCs) are considered one of the most promising fuel cell technologies for both stationary and mobile applications. Significant progress has been achieved over the past few decades. However, durability and cost have been identified as the top two issues in PEMFC technology. On the one hand, it is recognized that only when fuel cell costs are dramatically reduced to the US Department of Energy (DOE) target of \$50 kW^{-1} will fuel cells be competitive for virtually every type of power application. On the other hand, to reach technological readiness, automotive fuel cell power systems need to be as durable and reliable as today's internal combustion engines, corresponding to a 5000-h operating lifetime (approximately 7 months over a range of vehicle operating conditions, including variable relative humidity (RH), shutdown/start-up, freeze/thaw, and subfreezing down to $-40\,^{\circ}\mathrm{C}$), and stationary fuel cells must also meet operating lifetime targets of more than 40,000 h (approximately 4.5 years of continuous operation) to compete with extant distributed power generation systems, based on the 2015 DOE targets at component, stack, and system levels [1]. The DOE durability targets for stationary and transportation fuel cell applications stand on the lifetimes of energy conversion devices that are competitive with fuel cells, such as microturbines and internal combustion engines, respectively. However, currently the lifetimes of fuel cell vehicles and stationary cogeneration systems are around 1700 h and 10,000 h, respectively [2]. Clearly, intensive R&D is still needed to address the issues related to PEMFC durability or degradation in order to achieve sustainable commercialization.

As fuel cells must operate over a wide range of operating and cycling conditions, including temperatures from well below freezing to well above the boiling point of water, relative humidity (RH) from ambient to saturated, and half-cell potentials from 0 to >1.5 V, performance degradation is unavoidable, especially for transportation applications. Although the lifetime targets for automobiles are much lower than those for stationary applications, operating conditions such as dynamic load cycling, start-up/shutdown, and freezing/thawing make the target very challenging for current fuel cell technologies. The cell/stack conditions cycle, sometimes quite rapidly, between high and low voltage, temperature, humidity, and gas composition. The cycling results in physical and chemical changes to components, sometimes with catastrophic results [3]. Although performance degradation is unavoidable, the degradation rate can be minimized given a comprehensive understanding of degradation and failure mechanisms. Normally, degradation targets require less than 20% loss in the efficiency of the fuel cell system by the end of its life, and a degradation rate of 2–10 $\mu\mathrm{V\,h}^{-1}$ is commonly accepted for most applications [4].

To date, various failure modes have been identified, for example, catalyst particle ripening (particle coalescence), preferential alloy dissolution in the catalyst layer, carbon support oxidation (corrosion), catalyst poisoning, membrane thinning and pin-hole formation, loss of sulfonic acid groups in the ionomer phase of the catalyst layer or in the membrane, bipolar plate surface film growth, hydrophilicity changes in the catalyst layer and/or gas diffusion layer (GDL), and PTFE decomposition in the catalyst layer and/or GDL. Component decay or failure is affected by many internal and external factors, including material properties, fuel cell operating conditions (such as humidification, temperature, cell voltage, etc.), impurities or contaminants in the feeds, environmental conditions (e.g., subfreezing or cold start), operation modes (such as start-up, shutdown, potential cycling, etc.), and the design of the components and the stack. In addition, the degradation processes of different components are often interrelated in a fuel cell system. It is therefore important to separate, analyze, and systematically understand the degradation phenomena of each component so that novel component materials can be developed and novel designs for cells/stacks can be achieved to mitigate insufficient fuel cell durability.

In this ongoing R&D, long-term durability tests are often required to evaluate the degradation mechanisms of various components and the corresponding fuel cell systems. However, it is generally impractical and costly to operate a fuel cell under its normal conditions for several thousand hours, so accelerated stress test (AST) methods are preferred to facilitate rapid learning about key durability issues. The goal of the AST is to determine the durability and performance of current fuel cell components without having to test over many years [5]. Therefore, AST protocols are developed to ensure that the type and format of the data generated are sufficient so that the data sets can be compared, merged, and scaled. As new materials continue to be developed and new designs emerge, the need for relevant accelerated testing, as well as AST protocols, increases. However, as stated by Dillar et al. [6], it is difficult at this time to propose an accelerated protocol without performing a detailed examination of the existing fuel cell performance and diagnostics data, such as ionic resistance, polarization curves, lifetime tests, fuel crossover rates, and effluent concentrations. Also, regardless of the accelerated protocol developed, care must be taken to perform accelerated testing under conditions that do not introduce new failure mechanisms that would be unrealistic in fuel cell environments.

The intent of this review is to gather available information on AST methods and degradation test protocols for PEMFCs, providing practitioners with a useful toolbox for studying durability issues, in the hope that these protocols will help to prevent the prolonged test periods and high costs associated with real lifetime tests, to assess the performance and durability of PEMFC components, and to ensure that the generated data can be compared. It should be pointed out that although a variety of cell durability test standards have been developed by different organizations around the world, e.g., the Fuel Cell TEsting and STandardisation thematic NETwork (FCTESTNET) and the Japan Automobile Research Institute (JARI), the DOE AST methods are the most commonly accepted protocols. Therefore, this paper will mainly review AST protocols developed by the DOE programs, as well as AST protocols published in the open literature. For clarity, these testing protocols are summarized into two general categories—component level, and stack and system level. Within the component ASTs, electrocatalyst, catalyst support, membrane, GDL, ionomer, and interfacial degradation are included. At the system level, driving cycle is discussed.

2. A brief review of PEMFC degradation

2.1. Catalyst layer degradation

The catalyst layer (CL) is a multiple-phased matrix containing a high surface area carbon support loaded with nanoscaled Pt or Pt-alloy particles and ionomer recast dispersion. The thin CL, with a thickness in the order of ~15 μm, is critical for facilitating a fast catalytic reaction that requires free access for gas, electrons, protons, and water [4,7,8].

CL degradation relates to the stability of both the materials and the structure. Among other degradation phenomena (such as cracking or delamination of the CL, catalyst washout, electrolyte (ionomer) dissolution, carbon coarsening, and catalyst poisoning by contaminants), Pt particle growth, Pt migration, and carbon corrosion are considered the most dominant causes of CL degradation.

Several mechanisms have been proposed to account for Pt particle growth. Small Pt particles may dissolve and redeposit on the surface of larger particles, leading to particle growth, a phenomenon called Ostwald ripening [9]; random cluster–cluster collisions of Pt particles may result in Pt agglomeration on the carbon support at the nanoscale [10]; the minimization of the catalyst clusters' Gibbs free energy may lead to Pt particle growth at the atomic scale [11]; and the movement and coalescence of Pt particles on the carbon support can cause coarsening of the catalyst [12]. Particle size growth will result in reduction of the catalytically active surface area and ultimately lead to a decrease in catalyst activity and stability.

Pt migration occurs when the dissolved Pt species diffuse into the ionomer phase and subsequently precipitate in the membrane through the reduction of Pt ions by crossover hydrogen from the anode side [13–15]. Pt migration into the membrane dramatically decreases its stability and conductivity.

Carbon corrosion occurs through the electrochemical oxidation of carbon: $C+2H_2O \rightarrow CO_2+4H^+ +4e^-$ ($E^o = 0.207 V_{RHE}$) [16]. Despite carbon's thermodynamic instability, carbon corrosion during normal fuel cell operation is negligible at potentials lower than 1.1 V vs. RHE, due to its slow kinetics [17–19]. However, the presence of Pt can catalyze the carbon oxidation reaction and reduce its potential to 0.55 V vs. RHE or lower [20]. Carbon corrosion is believed to be promoted by the transition between start-up and shutdown cycles and by fuel starvation. Start-up and shutdown cause non-uniform distribution of fuel on the anode and hydrogen crossover through the membrane. Under circumstances of non-uniform fuel distribution and fuel starvation, the anode electrode is partially covered with hydrogen, making the anode potential negative and thus leading to carbon corrosion.

2.2. Membrane degradation

As a key component of the MEA, the membrane transports protons in the form of an electrolyte and acts as a barrier between anode and cathode to prevent gas permeation. The most commonly used membrane is composed of perfluorosulfonic acid (PFSA), such as Nafion® membranes.

Extensive studies have been conducted on membrane degradation mechanisms, and it is known that typical membrane degradation in a fuel cell results from mechanical, thermal, and chemical degradation. Mechanical degradation includes membrane cracks, tears, punctures, and pinholes due to the presence of foreign particles or fibers introduced during the MEA fabrication process that might perforate the membrane [21–23]. Chemical degradation originates from chemical attack by hydrogen peroxide radicals, resulting in breakage of the membrane's backbone and side-chain groups and subsequent loss of mechanical strength and proton conductivity, thus leading to an increase in resistance and declining cell performance [24–26]. Thermal degradation occurs when the membrane becomes dehydrated due to high-temperature operation, low humidity, and other causes, and leads to the loss of proton conductivity [27].

2.3. GDL degradation

The GDL is a carbon-based porous substrate between the CL and the flow field that enables gas phase transport, water transport, electronic and thermal conduction, and mechanical support. The GDL consists of two layers, a macro-porous layer made of carbon fiber paper or carbon cloth that is covered with a micro-porous layer (MPL) made of carbon black powder and a hydrophobic agent (PTFE). To date, the GDL is the least studied MEA component in terms of durability and degradation. Several GDL degradation mechanisms have been proposed: carbon oxidation [28,29], PTFE decomposition [30], and mechanical degradation as a result of compression [31]. The first two mechanisms cause hydrophobicity loss and changes in the GDL pore structure, resulting in an increase in the water content of the GDL and MPL and thus impeding gas phase mass transport [32–34]. It should be noted that the carbon fibers of the GDL and the carbon black particles of the MPL are more stable than the carbon black in the CL due to the absence of Pt that can catalyze the electrochemical oxidation of carbon. However, chemical surface oxidation of carbon by water cannot be excluded [28,29].

2.4. Bipolar plate degradation

Bipolar plates are responsible for separating the fuel and air (oxygen) gases and the coolant, uniformly distributing reactant and product streams, and collecting the current generated through the electrochemical reactions in the anode and cathode. Low ohmic resistance, low gas permeability, high corrosion resistance, good thermal and chemical stability, and appropriate mechanical properties are required for the long-term stability of the bipolar plates in an operating fuel cell environment [35,36]. Several materials have been employed and evaluated as bipolar plates for PEMFCs, including graphite, metals, graphite/carbon-based composites, and polymer-based composites [37–39]. Graphite and graphite composites have favorable properties such as high resistance to corrosion and chemicals, low density, and high electrical and thermal conductivity, but suffer from surface carbon oxidation/corrosion under extreme operating conditions such as cell reversal [4], leading to increased contact resistance. Metallic bipolar plates, depending on the nature of the metals, can suffer from corrosion and surface oxide film growth [40], leading to the release of contaminants and increased contact resistance [41,42].

2.5. Other component degradation

In comparison to the extensive studies on the durability of the key components (catalyst, membrane, GDL, and bipolar plates), durability studies on seals, endplates, and bus plates have long been ignored, and the literature data is very limited.

Gaskets can experience reduced thickness over long-term operation, leading to increased compression force on the GDL and a subsequent decrease in GDL porosity as well as an increase in reactant transport resistance [43]; gaskets can also experience crossover leakage, causing damage to the membrane [44]. Endplates and bus plates may suffer from similar corrosion issues but to a much lesser extent.

2.6. Operating conditions, environment, contamination, operation mode, and design-induced degradation

The durability of each component of a PEMFC is affected by many external factors in an operating fuel cell, including the fuel cell operating conditions (such as humidification, temperature, cell voltage, etc.), impurities or contaminants in the feeds, environmental conditions (e.g., subfreezing or cold start), operation modes (such as start-up, shutdown, potential cycling, etc.), and the design of the components and the stack [45,46].

The changes in temperature and RH associated with transitions between low and high power can have adverse effects on component properties and thus on the integrity of the fuel cell system. For example, as RH increases, the water uptake in the membrane increases and the ionomer swells, yielding tensile residual stresses during drying and thus contributing to mechanical failures in the membrane [47].

Impurities such as CO and H_2S are present in the fuel as a result of the reforming process, or in the air intake (e.g., NO_x, SO_x, or volatile organic compounds) due to air pollution [48]. Impurities can also come from fuel cell components (such as metal ions from bipolar plates) [49] or from the second elements in Pt alloy catalysts (such as Co^{2+}) [50,51]. These impurities are known to adversely affect fuel cell performance and durability by several means: the kinetic effect, caused by the poisoning of both anode and cathode catalyst sites; the mass transfer effect, due to changes in the structure and hydrophobicity of the CLs and/or GDLs; and the conductivity effect, caused by increased resistance in the membrane and ionomer [52].

The ability to survive and start up at subfreezing temperatures is an important requirement for PEMFCs, particularly in automobile applications. Subjecting a PEMFC to subfreezing temperatures has been reported to cause significant drops in the cathode electrochemical surface area (ECSA), which was attributed to ice formation in the CLs that resulted in increased porosity and ultimate delamination of the CL from the membrane [53]. The effect of freeze/thaw thermal cycles on the properties of MEA components (CL, GDL, and membrane) has been extensively studied but mostly through ex situ investigations, and the results are sometimes conflicting. Generally, freeze–thaw cycling will change the water content/state in the CLs [53], the air permeability of the GDL [31], and the conductivity of the membrane [54,55]. Detailed characterization of the durability of MEA components under fuel cell operating conditions during freeze/thaw cycles apparently needs to be better evaluated [45].

The design of fuel cell components such as flow fields and manifolds can have a significant impact on water management and feed flows, which can in turn affect the durability of MEA components and of the fuel cell. For example, an improper design in the channel depth of the flow fields can induce water blockage, and improper manifold design can result in poor cell-to-cell flow distribution, both of which will cause localized fuel starvation [56]. This localized fuel starvation can induce, through "reverse current" mechanisms, local potentials on the air electrode significantly higher than 1.0 V and thereby induce corrosion of the carbon support, resulting in permanent loss of electrochemically active area.

Fuel cell start-up and shutdown are operational modes that can have a profound influence on fuel cell durability. Under conditions of prolonged shutdown, all the hydrogen will eventually cross over from the anode to the cathode, resulting in the anode flow channels being filled with air. In this case, fuel cell start-up will create a transient condition in which fuel exists at the inlet but the outlet is still fuel-starved at the anode side. This localized fuel starvation can induce the local potential at the cathode to be higher than 1.8 V, causing serious deterioration in fuel cell performance and durability [57].

3. Accelerated stress test protocols for cell components

A fuel cell is a complicated system comprising various components. An AST should not only activate the targeted failure mode of the specific component, but also minimize the confounding effects from other components. Specific AST conditions and cycles are thus intended to isolate effects and failure modes, and are based on assumed, but widely accepted, mechanisms. For instance, the AST protocol for catalyst supports is different from the protocol for electrocatalysts because the components experience different degradation mechanisms under different conditions. Similarly, the AST for mechanical degradation of the membrane should isolate the effects of chemical degradation of the membrane.

To understand degradation mechanisms, component interactions, and the effects of operating conditions, and to increase sample throughput and reduce experimental time, fuel cell developers have implemented various ASTs to analyze the failure modes of current fuel cell components. These ASTs attempt to ensure that the test conditions and procedures do not result in degradation mechanisms that are different from those encountered during normal operation. The DOE and the US Fuel Cell Council (USFCC) have established PEMFC durability testing protocols with the intent of providing a standard set of test conditions and operating procedures for evaluating new cell component materials and structures. The DOE AST protocols were developed by the FreedomCAR Fuel Cell Technical Team (FCTT), comprised of representatives from the DOE and US automakers, to provide guidance and standardization for DOE component development projects. The FreedomCAR targets [58] are closely aligned with the DOE system, stack, and component technical targets. Input was also solicited and received from several fuel cell developers and from the USFCC, which is developing ASTs for broader, long-term applications. Basically, the USFCC protocols are in agreement with the DOE protocols. Other than the DOE and USFCC protocols, a variety of ASTs at different levels under various operating conditions have been published. Some are in line with the DOE protocols while others are specially designed for different purposes.

The following sections summarize the DOE cell component AST protocols, including for electrocatalysts, catalyst supports, membrane/MEA chemical stability, and membrane/MEA mechanical durability, derived from references [59,60], as well as examples of ASTs available in the literature.

3.1. *Electrocatalyst*

Electrocatalyst degradation mechanisms depend on factors such as potential, temperature, humidity, contaminants, and carbon support stability. Hence, electrocatalyst degradation can be accelerated by potential control, undesirable temperatures and humidities, contaminants, and load cycling [8]. In particular, at high electrode potentials the durability of catalysts can be compromised by Pt sintering, particle growth, and dissolution. AST stressors can be any combination of these factors when testing is conducted in a complex environment.

Because catalyst sintering/dissolution is accelerated under potential cycling [61], the DOE electrocatalyst AST is based on potential cycling. Table 1 lists the DOE testing protocols as well as the testing metrics for electrocatalysts [3]. Here catalytic activity is characterized in A mg^{-1} at 150 kPa absolute backpressure and at 900 mV with iR-corrected on H_2/O_2.

The AST for electrocatalyst specifies load cycling from 0.7 V to 0.9 V for 30,000 cycles or until catalytic activity loss reaches 60%, the ECSA decreases by 40%, or performance is reduced by 30 mV at 0.8 A cm^{-2}. Cycling to higher voltage would accelerate degradation but might also increase corrosion of the carbon support, convoluting interpretation of the results.

The USFCC presents two protocols for electrocatalyst testing. The first is very similar to the DOE protocol described in Table 1 but with a slightly wider voltage cycling range (0.6–0.96 V) and air on the cathode. The second has a still wider voltage cycling range (0.6–1.2 V) with N_2 on the cathode [62]. The DOE range is restricted to 0.7–0.9 V to reduce the possibility of catalyst support degradation at higher voltages and to isolate degradation effects.

A variety of investigations into catalyst degradation have been conducted [63–70]. Catalyst ASTs described in the literature generally simulate duty cycle induced catalyst degradation by potential cycling from a lower potential, in the range of 0.1–0.7 V, to increased potential, such as OCV, 1.0, or 1.2 V. Some examples of these studies are given in Table 2.

3.2. *Catalyst support*

Durability of catalyst supports is another technical barrier for stationary and transportation applications of PEMFCs. Conventional PEM electrodes consist of platinum particles supported on carbon. Carbon is an excellent material for supporting electrocatalysts, allowing facile mass transport of reactants and fuel cell reaction products, and providing good electrical conductivity and stability under normal conditions. However, under prolonged conditions of high temperature, high water content, low pH, high

Table 1
DOE AST protocols for electrocatalyst [3] (reproduced with permission from the Electrochemical Society).

Cell	Single cell 25–50 cm^2	
Operating con- di- tions	Temperature: 80 °C Relative humidity: anode/cathode 100/100% Fuel/oxidant: H_2/N_2 Pressure: 150 kPa absolute	
Cycle	Step change: 30 s at 0.7 V and 30 s at 0.9 V Cycle time: 60 s Cycle number: 30,000	
Metrics	Catalytic activity	Frequency: beginning and end of life Target: <60% loss of initial catalytic activity
	Polarization curve	Frequency: after 0, 1k, 5k, 10k, and 30k cycles Target: <30 mV loss at 0.8 A cm^{-2}
	ECSA/cyclic voltammetry	Frequency: after 1, 10, 30, 100, 300, 1000, 3000 cycles and every 5000 cycles thereafter Target: <40% loss of initial area

Table 2
Catalyst/CL AST protocols in the literature.

Test mode	Stressor	Available protocols	Authors	Reference
In situ	Potential cycling	Linear potential sweep from 0.1 V to an upper limit (varying from 0.8 V to 1.5 V) at 10 mV s^{-1} in increments of 300 cycles; 80 °C, N_2 with 226% RH at the cathode, H_2 with 100% RH at the anode	R.L. Borup et al.	[71]
Ex situ	Fixed potential	20 °C, 0.5 M H_2SO_4, a fixed potential at 1.2 V (vs. RHE) for 192 h	Y.Y. Shao et al.	[72]
Ex situ (Pt dissolution)	Constant potential	40–80 °C, 1 M $HClO_4$, constant potential between 0.85 V (vs. RHE) and 1.4 V (vs. RHE)	V.A.T. Dam et al.	[73]
In situ	Potential cycling	Linear sweep from 0.1 to either 1.0 or 1.2 V at 10 mV s^{-1}; 60 °C or 80 °C, 50% or 100% RH, N_2 on the cathode and H_2 on the anode	K.L. More	[74]
In situ	Potential	Cathode 1.2 V relative to the anode; 80 °C, 100% RH, N_2 on the cathode and H_2 on the anode	J. Frisk et al.	[75]

oxygen concentration, and/or high potential, oxidation of carbon (carbon corrosion) is prone to acceleration. Corrosion of high surface area carbon supports at high electrode potentials poses significant concerns and is typically accelerated during fuel starvation and start-up/shutdown cycling. Evaluation of carbon support durability is thus performed at high voltage with hydrogen on the anode and nitrogen on the cathode to isolate electrochemical corrosion from chemical corrosion in the presence of air. Table 3 lists the DOE AST protocols as well as the testing metrics for catalyst supports [3].

The AST for the support specifies a steady-state hold at 1.2 V for 200 h or until catalytic activity loss reaches 60%, ECSA decreases by 40%, or performance is reduced by 30 mV at 1.5 A cm^{-2} or at rated power. Supports other than carbon may require changes to the AST to reflect different degradation mechanisms.

The USFCC provides two test cycles for evaluating catalyst supports. One cycle uses the same hold voltage as the DOE (1.2 V) and the other uses 1.5 V to accelerate corrosion. Both USFCC protocols use lower temperature (80 °C vs. DOE's 95 °C) and higher RH (100% vs. DOE's 80%).

Other protocols used for catalyst support ASTs are similar to the DOE/USFCC ones, which are more or less related to high potential or to potential cycling with high potential involved. Some examples are listed in Table 4.

3.3. Membrane

Accelerated membrane tests can include undesirable temperature and RH, OCV, load cycling, Fenton's test, freeze/thaw cycling, stress cycling under tension, high-pressure testing, and high-temperature exposure [8].

3.3.1. Membrane mechanical AST

Membranes are the key components of the fuel cell MEA and stack; they must be durable and tolerate a wide range of operating conditions, including humidity ranging from ambient to 100% RH and temperature ranging from −40 to 120 °C. Improved membranes are needed that perform better and are less expensive than the current generation of polymer membranes.

Table 3
DOE AST protocols for catalyst support [3] (reproduced with permission from the Electrochemical Society).

Cell	Single cell 25–50 cm^2	
Operating conditions	Temperature: 95 °C Relative humidity: anode/cathode 80/80% Fuel/oxidant: H_2/N_2 Pressure: 150 kPa absolute	
Cycle	Step: hold at 1.2 V Cycle time: 24 h Total time: 200 h	
Metrics	CO_2 release	Frequency: on-line Target: <10% mass loss
	Catalytic activity	Frequency: every 24 h Target: <60% loss of initial catalytic activity
	Polarization curve	Frequency: every 24 h Target: <30 mV loss at 1.5 A cm^{-2} or rated power
	ECSA/cyclic voltammetry	Frequency: every 24 h Target: <40% loss of initial area

Table 4
Catalyst support AST protocols in the literature.

Test mode	Stressor	Available protocols	Authors	Reference
In situ	Potential cycling	Potential cycling from 0.04 to 1.2 V vs. RHE at 2 mV s^{-1}; 50 °C, with fully humidified 4% H_2/N_2 and He for the anode and cathode, respectively	L.M. Roen et al.	[20]
In situ	Idle and OCV	Idle (0.9 V vs. RHE) and OCV for 2000 h at 80 °C	R. Makharia et al.	[76]
In situ	Potential cycling	Linear potential sweep from 0.1 to 0.96 V, 1.0 V, 1.2 V, and 1.5 V	R.L. Borup et al.	[71]

Mechanical and chemical degradation of the polymer ionomer that comprises the PEM both increase with temperature. Change in RH is another serious condition that results in mechanical degradation of the membrane during practical operation. RH cycling results in swelling of the membrane as it absorbs water at high RH and shrinkage as it loses water at low RH. This swell/shrink cycling results in high mechanical stresses in the membrane and subsequent mechanical failure, leading to gas crossover through the membrane. As demonstrated by Crum and Liu [77], RH cycling can be used to examine mechanical durability in isolation, or to examine combined mechanical and chemical durability. In an inert nitrogen atmosphere with RH cycling, the mechanical durability associated with expansion and contraction of the ionomer under the flow field channels is isolated. When the same RH cycling is employed with air and hydrogen feed gases, mechanical and chemical durability are combined. Table 5 shows the DOE membrane mechanical AST protocols based on RH cycling [3]. The test continues for 20,000 cycles or until crossover is 10 sccm. Membrane performance is measured as the number of cycles before a threshold crossover is observed.

Gas crossover is a good indicator to monitor membrane degradation or mechanical stability. This can be done by either measuring gas flow rate according to the procedures developed by the USFCC or measuring hydrogen crossover electrochemically (mA cm^{-2}), the latter being well accepted by fuel cell researchers.

3.3.2. *Membrane chemical AST*

The DOE AST protocol for membrane chemical durability involves a steady-state hold for 200 h at OCV and 90 °C, as listed in Table 6 [3]. At OCV, the fuel and oxidant are not being consumed electrochemically, so there is potentially more crossover, resulting in peroxide production and radicals that attack the membrane [78]. Similarly, crossover can be measured by either gas flow rate or hydrogen crossover. The test continues until OCV decays by 20% or crossover reaches 20 mA cm^{-2}. Fluoride ion release (or an equivalent for non-fluorinated membranes) is also measured during the test for monitoring purposes. Fluoride ion release is an indication of membrane deterioration for fluorinated membranes and has been correlated to membrane life [79,80].

The USFCC ASTs for membranes are virtually identical to the DOE protocols described in Tables 3 and 4. The differences are associated with the oxygen concentration (air vs. the USFCC's 40% or 100% O_2) on the cathode during the test. The DOE specifies air to accommodate those laboratories that restrict oxygen usage.

Unfortunately, membrane durability is always studied using a MEA. Thus, the DOE/USFCC membrane AST protocol is described as a membrane/MEA AST protocol. Despite the difficulties, several studies have examined candidate conditions for ex situ accelerated testing of membranes. LaConti et al. [21] describe multiple methods of accelerating degradation in membranes. It is possible to simulate the degradation of PEMs using an accelerated test medium such as Fenton's reagent (small amounts of hydrogen peroxide (∼3%) and Fe^{2+} ions (4 ppm) in solution). This Fenton's test is also described by the USFCC as an additional membrane/MEA protocol. The ferrous ion catalyzes the decomposition of peroxide to peroxy and/or hydroxyl radicals that chemically attack the perfluorinated sulfonic acid polymers. Measurement of F^- in the effluent provides a measure of membrane stability [80]. However, this Fenton's test only applies to fluorine membranes, such as Nafion®. Another additional membrane/MEA AST protocol recommended by the USFCC is a combined humidity/load cycle developed by DuPont. The RH is cycled between 1 and 100% at fixed load for 24 h, followed by a load cycle between 10 and 800 mA cm^{-2} at fixed RH for 24 h. The cycle is repeated for the duration of the test. The DOE did not include this protocol because although it provides insight into the behavior of a membrane with the combined cycle, it does not allow isolation of the effects and degradation mechanisms for RH and voltage cycling.

W.L. Gore & Associates have conducted extensive investigations into durability testing and accelerated testing procedures. They observed an approximately 10× relationship for membrane life between their standard and accelerated residential test procedures, while H_2 crossover (monitored regularly for both standard and accelerated testing) gradually increased over time. Compared to the standard protocol (T_{cell} = 70 °C, DP_a, DP_c = 70 °C, $P_{H2} = P_{Air}$ = 0 psig), they concluded that the accelerated fuel cell life test protocol (T_{cell} = 90 °C, DP_a, DP_c = 83 °C, P_{H2} = 5 psig, and P_{Air} = 15 psig) was a valid testing condition to evaluate membrane durability for residential fuel cell applications [81].

Numerous experiments have tackled membrane degradation [82–88], examining various stressors: temperature, humidity, freeze–thaw cycling, OCV, and Fenton's test. Some examples of membrane ASTs, as well as their testing protocols, are listed in Table 7.

3.4. *GDL*

Changes in the microstructure and surface characteristics of the GDL due to material loss and pore size distribution shifts may cause changes in the water content level and transport properties of the

Table 5
DOE AST protocols for membrane mechanical degradation [3] (reproduced with permission from the Electrochemical Society).

Cell	Single cell 25–50 cm^2 (test using a MEA)	
Operating conditions	Temperature: 80 °C Fuel/oxidant: air/air at 2 slpm on both sides Pressure: ambient or no back-pressure	
Cycle	Step change: cycle 0% RH (2 min) to 90 °C dewpoint (2 min) Cycle time: 24 h Total time: until crossover >10 sccm or 20,000 cycles	
Metrics	Crossover	Frequency: every 24 h Target: <10 sccm

Table 6
DOE AST protocols for membrane chemical stability [3] (reproduced with permission from the Electrochemical Society).

Cell	Single cell 25–50 cm^2	
Operating conditions	Temperature: 90 °C Relative humidity: anode/cathode 30/30% Fuel/oxidant: hydrogen/air at stoics of 10/10 at 0.2 A cm^{-2} Pressure: anode 250 kPa (inlet), cathode 200 kPa (inlet)	
Cycle	Step: steady state OCV Cycle time: 24 h Total time: 200 h	
Metrics	F-release or equivalent for non-fluorine membranes	Frequency: at least every 24 h
	Hydrogen crossover (mA cm^{-2})	Frequency: every 24 h Target: <20 mA cm^{-2}
	OCV	Frequency: continuous Target: <20% loss in OCV
	High-frequency resistance	Frequency: every 24 h at 0.2 A cm^{-2}

MEA. To date, the DOE has not developed any standard AST protocols on durability and degradation issues for GDLs. Even in the literature, only a limited number of studies have focused on GDLs as effective characterization techniques is relatively limited. As a result, no DOE or other commonly used AST protocols are available for this review. Instead, a brief summary of some in situ and ex situ stressors that have been used to tackle GDL degradation is provided.

In situ stressors that have been used to assess GDL stability include freeze/thaw cycles and fuel starvation. For example, Kim et al. [92] reported interfacial delamination between the CL and GDL after 100 freeze/thaw cycles from −40 °C to 70 °C, which resulted from ice formation and in turn significantly increased GDL deformation. Mukundan et al. [93] conducted freeze/thaw cycles down to −80 °C using dry ice, and their results indicated that multiple cycles could lead to interfacial delamination and GDL failure in the fuel cell. Also, prolonged or repeated pulses of H_2 starvation and high potential control can change the microstructure and cause material loss in the MPL and GDL. Oszcipok et al. [94] have observed reduced GDL surface hydrophobicity in cold-start conditions.

Many research studies have also examined GDL degradation using ex situ methods. In durability tests, ex situ stressors help avoid potential confounding effects from other adjoining components. Ex situ stressors are intended to simulate a complex environment for the GDL during fuel cell operation. For example, Frisk et al. [95] submerged the GDL in hydrogen peroxide solution, a method similar to Fenton's test, and in this way detected weight loss and MPL contact angle increase in the GDL. Wood et al. [96] immersed GDL samples in liquid water with different oxygen concentrations to look at decreases in hydrophobicity with exposure time and water temperature. Compressive strain of the GDL under steady-state and freezing conditions was also used as an ex situ stressor by Lee and Merida [31]. By monitoring the GDL's properties – e.g., electrical resistivity, bending stiffness, air permeability, surface contact angle, porosity, and water vapor diffusion – they were able to investigate the degradation mechanisms.

Researchers at the Institute for Fuel Cell Innovation (IFCI) of the National Research Council Canada (NRC) [97–99] have established their own GDL testing protocols. Prioritization of the various stressors was accomplished by exposing samples of GDL to elevated conditions for 200 h. Each stressor was applied individually at an elevated level to isolate the particular effect of the stressor under examination. The list of stressors was trimmed to four in order to accommodate the 200 h of testing required for each during the first quarter. The four stressors were:

- Elevated flow rate
- Elevated temperature (120 °C)
- Constant electrical potential (1.8 V)
- Dynamic electrical potential

Early on, it was proposed that GDL damage during hot-pressing or stack assembly at overly high pressures could have an effect on degradation. The conditions selected to represent the two types of damaged GDL were:

- Hot-pressing in a hot press at 135 °C and 30 bar for 5 min
- Stack assembly in a cell with a bladder pressure of 200 psig for 30 min

To accommodate the damaged GDL samples into the stressor testing, a 3-cell stack was required rather than the single cell originally planned for. A 3-cell stack allowed for simultaneous testing of an undamaged GDL sample and both damaged GDL samples under identical conditions.

Upon completion of the testing at elevated conditions, the test plan called for characterization of the induced degradation. Characterization was accomplished through multiple sets of polarization curves acquired using a catalyst-coated membrane (CCM) in single cell hardware. Characterization was also accomplished through the use of various analytical techniques, such as mass loss and SEM. Additional recommended tools are:

Table 7
Membrane/MEA AST protocols in the literature.

Test mode	Stressor	Available protocols	Authors	Reference
In situ	RH cycling	65 °C, RH cycling from 30 to 80% or from 80 to 120% with 30 min/step, with air supplied to the anode and the cathode	X. Huang et al.	[89]
In situ	RH cycling	80 °C, RH cycling from 0 to 150% with 2 min/step, with air supplied to the anode and the cathode	M.F. Mathias et al.	[59]
In situ	OCV	OCV at cell temperature of 80 °C and both gases humidified at 60 °C, with hydrogen and air supplied to the anode and the cathode	M. Inaba et al.	[90]
Ex situ	Fenton's test	Solution method: 16 mg L^{-1} Fe^{2+} in a solution of $FeCl_2/4H_2O$ and 30%H_2O_2; 72 °C; fresh solution every 12 h. Exchange method: Nafion® samples were treated in saturated $FeCl_2{\cdot}4H_2O$ solution for 24 h, then 40 mL of peroxide was added. 72 °C; fresh peroxide every 24 h	S. Kundu et al.	[91]

- Contact angle analysis
- X-ray diffraction
- X-ray photoelectron spectroscopy
- Mercury intrusion porosimetry
- Surface roughness (Wyko 3-D Surface Profiler, model NT-2000)
- TGA

3.5. *Ionomer in the CL*

Many research groups have postulated that ionomer degradation/loss might be one of the critical factors leading to reduced CL performance after long-term operation or AST. As the actual Nafion® ionomer network within the CL is not as easily distinguished/imaged as Pt and carbon supports, it is usually difficult to identify ionomer degradation in the CL using traditional morphology characterization methods. However, some research groups have recently made remarkable progress in confirming Nafion® ionomer degradation in CLs by using unique diagnostic tools. Xie et al. [63] used cell impedance trends to reveal degradation of the recast ionomer network in the CL. Zhang et al. [100] used XPS to detect CL ionomer degradation (or decrease in concentration). With EIS, Hou et al. [101] measured the CL's ionic resistance at different currents to monitor changes in the ionic resistance profile. With the help of statistical information from experimental images of CLs, Rong et al. [102] simulated the CL microstructure, revealing microstructural changes on the microscale during PEMFC ageing.

An additional consideration is that as ionomer degradation in the CL is always coupled with membrane degradation, it is difficult to distinguish them from each other, for example by measuring fluoride release rate. Researchers at the University of Waterloo, working with researchers at the NRC, have considered using hydrocarbon membranes to investigate ionomer degradation in the catalyst layer. The use of hydrocarbon membranes helps eliminate the effects of membrane degradation. A preliminary testing protocol for this purpose combines various stressors, as shown in Table 8.

4. Cell/stack durability test protocols

Component degradation protocols are important in evaluating PEMFC durability at the material and component level with the intent to understand and compare the degradation mechanisms of different materials/components, and thus to improve the component's performance and durability, particularly for the development of new materials and new designs. In a single cell or stack, many components have strong and complex interactions, complicating the degradation mechanisms of particular components at the cell or stack level. Therefore, each component must ultimately be evaluated in an integrated fuel cell or stack system so that the durability data of each component can more accurately reflect the component's lifetime in an actual fuel cell of a real stationary power generator or vehicle. This section summarizes the degradation/durability testing protocols that have been developed or used for single cells or stacks. It has to be noted that the existing single cell/stack degradation testing protocols may not be comprehensive enough to evaluate the effects of all operating conditions that will be encountered during real fuel cell operation, particularly for automobile applications, which often involve a combination of various complicated situations. More comprehensive protocols need to be developed to address additional issues.

4.1. *US DOE single cell/stack testing protocols for transportation applications*

The US DOE, through its multiple-year Hydrogen Program, has developed durability testing protocols for fuel cell stacks.

Steady-state durability tests [103] are conducted under steady-state conditions (constant voltage and constant current) for a period of time, sometimes as long as a few thousand hours. These tests aim to examine the degradation rate of a single cell/stack and the degradation mechanisms of components under steady-state conditions. Measurements of polarization curves, membrane resistance, hydrogen crossover, and electrochemical surface area (through CVs) are made in situ periodically during the durability test to characterize changes in those fundamental properties as a function of time. Effluent water analysis (elemental analysis, ionic content, and pH) is conducted to monitor for degradation products. Changes in the CL (catalyst particle size, catalyst sintering, carbon corrosion, etc.) and the membrane are characterized after the durability tests by scanning electron microscopy/energy dispersive X-ray spectroscopy (SEM/EDS), X-ray fluorescence (XRF), X-ray diffraction (XRD), transmission electron microscopy (TEM), and neutron scattering, etc.

Potential cycling durability tests are applied to single cells as an accelerated testing technique to mimic the dynamic load of an automotive application, which requires many rapid changes in load over the course of the fuel cell's lifetime [103]. During potential cycling (sweeping), the anode is exposed to nitrogen. The cathode potential is swept linearly from an initial voltage of usually 0.1 V to an upper limit voltage ranging from 0.96 V to 1.2 V. The scanning rate ranges from 5 to 50 mV s^{-1}. After cycling intervals, the polarization curve of the MEA and the catalyst surface area are measured. After the cycling is completed, post-characterization measurements are performed by XRD, SEM, TEM, and other methods, as described earlier. These post mortem analyses are used to differentiate the contributions of fuel cell components to the degradation of the overall cell performance.

Start-up/shutdown cycling durability tests [104] have been developed by Los Alamos National Lab (LANL) to examine the degradation of fuel cell components when the fuel cell is subjected to shutdown/start-up cycles. In this protocol, for shutdowns the fuel cell is first run at OCV with continuous dry air flow at the cathode side, then purged at the anode side with dry air for 5 min; for start-ups, the anode is subjected to dry hydrogen flow at full power for 5 min. In addition to the post mortem analyses discussed earlier, another important analytical tool to determine the effect of start-up/shutdown is measurement of CO_2 (and CO) evolution at the cathode by non-dispersive infrared (NDIR).

Drive cycle tests [45,105] are protocols developed and standardized by the DOE to assess the long-term durability of fuel cells for vehicular applications and to compare stack performance with DOE targets. The drive cycle protocol was constructed by converting federal internal combustion engine drive cycle "US06" to an equivalent PEMFC engine drive cycle. This protocol involves stepping through a series of different current draws typical of automotive loads. To establish the current density profile, an initial polarization curve is plotted and then used to determine the current densities at which average cell voltages of 0.88, 0.80, 0.75, 0.65, and 0.6 V are obtained. The stack is then subjected to the current density profile shown in Table 9 [45]. The stack load cycle based on the initial stack polarization curve is shown in Fig. 1 [45]. As a quantitative measure, the stack durability is defined as the time it takes for the average cell voltage to decay by 10% from the initial voltage when tested according to the above procedures.

4.2. *Durability tests for stationary applications*

The DOE durability target for PEMFCs in stationary applications is much longer than for automotive applications (20,000 h vs. 5000 h by 2015). However, the operational complexity of stationary applications is far less. As a result, there have not been as many efforts to develop testing protocols for PEMFCs in sta-

Table 8
AST protocols for ionomer degradation in the CL using hydrocarbon membranes.

Test condition (1)	Idle condition (10 mA cm^{-2}), single cell 25–50 cm^2	
Step time	48 h	
Test condition (2)	Operational condition (300 mA cm^{-2})	
Step time	48 h	
Test condition (3)	Load cycling at 50, 400, and 800 mA cm^{-2}, 10 h for 2 cycles	
Step time	60 h	
Test condition (4)	Thermal cycling at 35, 55, 70, and 90 °C for 10 h each	
Step time	40 h	
Metric	F-release or equivalent for non-fluorine membranes	Frequency: at the end of each cycle or at least every 24 h
	Hydrogen crossover	Frequency: at the end of each cycle or at least every 24 h Target: <20 mA cm^{-2}
	Polarization curve	Frequency: at the end of each cycle or at least every 24 h
	High-frequency resistance	Frequency: at the end of each cycle or at least every 24 h

Table 9
Current density vs. time for the drive cycle profile [45] (reproduced with permission from Borup et al. [45]. Copyright {2007} American Chemical Society).

Step	Duration (s)	Cxx	Step	Duration (s)	Cxx
1	15	OCV	9	20	C_{75}
2	25	C_{80}	10	15	C_{88}
3	20	C_{75}	11	35	C_{80}
4	15	C_{88}	12	20	C_{60}
5	24	C_{80}	13	35	C_{65}
6	20	C_{75}	14	8	C_{88}
7	15	C_{88}	15	35	C_{75}
8	25	C_{80}	16	40	C_{88}

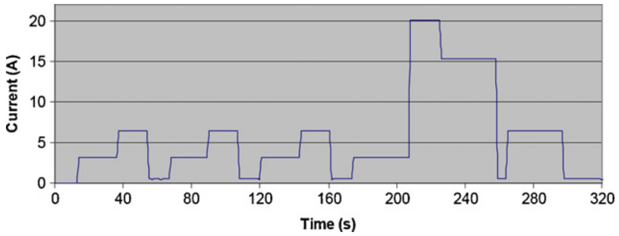

Fig. 1. Load profile for the stack drive cycle stress test [45] (reproduced with permission from Borup et al. [45]. Copyright {2007} American Chemical Society).

tionary applications. Most long-term lifetime tests for stationary applications are carried out at a given set point or group of set points with the voltage or, more commonly, the current density held constant for hundreds or thousands of hours per test [45]. The joint research council (JRC) has used four different sub-tests (normal efficiency test, thermal load cycling, electrical load cycling, and start-up/shutdown) in sequence for the stationary fuel cell system test module [106] as opposed to the single cell test module TM PEFC SC 5-4 [107], in which they utilized on/off cycling to accelerate ageing.

5. Concluding remarks

The US DOE hydrogen programs have established durability targets for PEMFCs in transportation and stationary applications. These targets are based on the characteristics of current and future competitive technologies. AST/durability protocols have been developed by the DOE and the FreedomCAR FCTT at the component level in an attempt to gain a measure of component durability and performance against DOE technical targets. These protocols have not been conclusively correlated to actual service, and are not intended to be comprehensive because many issues critical to a transportation fuel cell (e.g., freeze/thaw cycles) are not addressed due to the design-specific nature of operating procedures. As a result, the drive cycle protocol was constructed by converting the federal internal combustion engine drive cycle to an equivalent PEMFC engine drive cycle, which still requires correlation with data from stacks and systems operating under actual drive cycles. Therefore, additional tests to correlate these results with real world lifetimes may be needed, including actual driving, start/stop, and freeze/thaw cycles.

References

[1] Hydrogen, Fuel Cells & Infrastructure Technologies Program Multi-Year Research, Development and Demonstration Plan, August 2006 at http://www1.eere.energy.gov/hydrogenandfuelcells/mypp.
[2] T. Payne, Fuel Cells Durability & Performance, The Knowledge Press Inc., US Brookline, 2009.
[3] N.L. Garland, T.G. Benjamin, J.P. Kopasz, ECS Trans. 11 (2007) 923–931.
[4] J. Wu, X.Z. Yuan, J.J. Martin, H. Wang, J. Zhang, J. Shen, J. Power Sources 184 (2008) 104–119.
[5] DOE cell component accelerated stress test protocols for PEM fuel cells at http://www1.eere.energy.gov/hydrogenandfuelcells/fuelcells/components.html. March 2007.
[6] D.A. Dillar, S. Guo, M.W. Ellis, J.J. Lesko, J.G. Dillard, J. Sayre, B. Vijayendran, Fuel Cell Sci. Eng. Technol. (2004) 553–560.
[7] F.A. de Bruijn, V.A.T. Dam, G.J.M. Janssen, Fuel Cells 8 (2008) 3–22.
[8] S. Zhang, X.Z. Yuan, H. Wang, W. Merida, H. Zhu, J. Shen, S. Wu, J. Zhang, Int. J. Hydrogen Energy 34 (2009) 388–404.
[9] M. Watanabe, K. Tsurumi, T. Mizukami, T. Nakamura, P. Stonehart, J. Electrochem. Soc. 141 (1994) 2659–2668.
[10] Y. Zhai, H. Zhang, D. Xing, Z. Shao, J. Power Sources 164 (2007) 126–133.
[11] P. Ascarelli, V. Contini, R. Giorgi, J. Appl. Phys. 91 (2002) 4556–4561.
[12] M.S. Wilson, F.H. Garzon, K.E. Sickafus, S. Gottesfeld, J. Electrochem. Soc. 140 (1993) 2872–2877.
[13] T. Akita, A. Taniguchi, J. Maekawa, Z. Siroma, K. Tanaka, M. Kohyama, K. Yasuda, J. Power Sources 159 (2006) 461–467.
[14] P.J. Ferreira, G.J. la O', Y. Shao-Horn, D. Morgan, R. Makharia, S. Kocha, J. Electrochem. Soc. 152 (2005) A2256–A2271.
[15] J.X. Zhang, B.A. Litteer, W.B. Gu, H. Liu, H.A. Gasteiger, J. Electrochem. Soc. 154 (2007) B1006–B1011.
[16] D.P. Wilkinson, J. St-Pierre, in: W. Vielstich, H.A. Gasteiger, A. Lamm (Eds.), Handbook of Fuel Cells: Fundamentals, Technology and Applications, vol. 3, John Wiley & Sons Ltd., 2003, pp. 611–626.
[17] S.D. Knights, K.M. Colbow, J. St-Pierre, D.P. Wilkinson, J. Power Sources 127 (2004) 127–134.
[18] N. Sisofo, 4th Annual Inter. Fuel Cell Testing Workshop, Vancouver, BC, Canada, September 12–13, 2007.
[19] A. Taniguchi, T. Akita, K. Yasuda, Y. Miyazaki, J. Power Sources 130 (2004) 42–49.
[20] L.M. Roen, C.H. Paik, T.D. Jarvi, Electrochem. Solid-State Lett. 7 (2004) A19–A22.
[21] A.B. LaConti, M. Hamdan, R.C. McDonald, in: W. Vielstich, A. Lamm, H.A. Gasteiger (Eds.), Handbook of Fuel Cells, vol. 3, Wiley, Chichester, 2003, p. 647.
[22] G. Escobedo, K. Raiford, G.S. Nagarajan, K.E. Schwiebert, ECS Trans. 1 (2006) 303–311.
[23] C. Stone, G.H.M. Calis, 2006 Fuel Cell Seminar Abstracts, Courtesy Associates, Hawaii, 2006.
[24] O. Yamazaki, Y. Oomori, H. Shintaku, T. Tabata, 2005 Fuel Cell Seminar Abstracts, Courtesy Associates, Palm Springs, 2005.
[25] E. Endoh, 2005 Fuel Cell Seminar Abstracts, Courtesy Associates, Palm Springs, 2005.
[26] R. Miyoshi, Y. Sakiyama, Y. Miwa, Y. Aoki, T. Yamamoto, Y. Ueno, A. Masuda, Y. Nakagawa, G. Katagiri, H. Nakayama, M. Hori, 2006 Fuel Cell Seminar Abstracts, Courtesy Associates, Hawaii, 2006.
[27] T. Okada, in: W. Vielstich, A. Lamm, H.A. Gasteiger (Eds.), Handbook of Fuel Cells, vol. 3, Wiley, Chichester, 2003, pp. 627–646.
[28] D.A. Stevens, J.R. Dahn, Carbon 43 (2005) 179–188.
[29] M. Cai, M.S. Ruthkosky, B. Merzougui, S. Swathirajan, M.P. Balogh, S.E. Oh, J. Power Sources 160 (2006) 977–986.

[30] M. Schulze, N. Wagner, T. Kaz, K.A. Friedrich, Electrochim. Acta 52 (2007) 2328–2336.

[31] C. Lee, W. Merida, J. Power Sources 164 (2007) 141–153.

[32] L.R. Jordan, A.K. Shukla, T. Behrsing, N.R. Avery, B.C. Muddle, M. Forsyth, J. Power Sources 86 (2000) 250–254.

[33] U. Pasaogullari, C.Y. Wang, Electrochim. Acta 49 (2004) 4359–4369.

[34] A.Z. Weber, J. Newman, J. Electrochem. Soc. 152 (2005) A677–A688.

[35] V. Mehta, J.S. Cooper, J. Power Sources 114 (2003) 32–53.

[36] F. de Bruijn, Green Chem. 7 (2005) 132–150.

[37] J. Wind, A. LaCroix, S. Braeuninger, P. Hedrich, C. Heller, M. Schudy, in: W. Vielstich, H.A. Gasteiger, A. Lamm (Eds.), Handbook of Fuel Cells: Fundamentals, Technology and Applications, vol. 3, John Wiley & Sons Ltd, 2003, pp. 294–307.

[38] G.O. Mepsted, J.M. Moore, in: W. Vielstich, H.A. Gasteiger, A. Lamm (Eds.), Handbook of Fuel Cells: Fundamentals, Technology and Applications, vol. 3, John Wiley & Sons Ltd, 2003, pp. 286–293.

[39] D.J.L. Brett, N.P. Brandon, J. Fuel Cell Sci. Technol. 4 (2007) 29–44.

[40] F. Barbir, PEM Fuel Cell: Theory and Practice, Elsevier Academic Press, New York, 2005, pp. 99–113.

[41] L. Ma, S. Warthesen, D.A. Shores, J. New Mater. Electrochem. Syst. 3 (2000) 221–228.

[42] A. Pozio, R.F. Silva, M. De Francesco, L. Giorgi, Electrochim. Acta 48 (2003) 1543–1549.

[43] S.J.C. Cleghorn, J. Power Sources 158 (2006) 446–458.

[44] A. Husar, M. Serra, C. Kunusch, J. Power Sources 169 (2007) 85–91.

[45] R. Borup, J. Meyers, B. Pivovar, Y.S. Kim, R. Mukundan, N. Galand, et al., Chem. Rev. 107 (2007) 3904–3951.

[46] H.J. Wang, H. Li, X.Z. Yuan (Eds.), PEM Fuel Cell Failure Mode Analysis, CRC Press, Taylor & Francis Group, USA, 2011.

[47] A. Kusoglu, A. Karlsson, M.H. Santare, S. Cleghorn, W.B. Johnson, J. Power Sources 161 (2006) 987–996.

[48] H. Li, J.L. Zhang, K. Fatih, Z. Wang, Y. Tang, Z. Shi, et al., J. Power Sources 178 (2008) 103–117.

[49] H. Li, K. Tsay, H.J. Wang, J. Shen, S. Wu, N. Jia, et al., J. Power Sources 195 (2010) 8089–8093.

[50] H. Li, K. Tsay, H.J. Wang, S. Wu, J.J. Zhang, N. Jia, et al., Electrochim. Acta 55 (2010) 2622–2628.

[51] H. Li, J. Gazzarri, K. Tsay, S. Wu, H.J. Wang, J.J. Zhang, et al., Electrochim. Acta 55 (2010) 5823–5830.

[52] X. Cheng, Z. Shi, N. Glass, L. Zhang, J.J. Zhang, D.T. Song, Z.S. Liu, H.J. Wang, J. Shen, J. Power Sources 165 (2007) 739–754.

[53] E. Cho, J.J. Ko, H.Y. Ha, S.A. Hong, K.Y. Lee, T.W. Lim, et al., J. Electrochem. Soc. 150 (2003) A1667–A1670.

[54] M. Cappadonia, J.W. Erning, U. Stimming, J. Electroanal. Chem. 376 (1994) 189–193.

[55] A. Siu, J. Schmeisser, S. Holdcroft, J. Phys. Chem. B 110 (2006) 6072–6080.

[56] C.A. Reiser, L. Bregoli, T.W. Patterson, J.S. Yi, J.D. Yang, M.L. Perry, et al., Electrochem. Solid-State Lett. 8 (2005) A273–A276.

[57] J.P. Meyers, R.M. Darling, J. Electrochem. Soc. 153 (2006) A1432–A1442.

[58] FreedomCAR Fuel Cell Technical Team Roadmap at http://www.uscar.org/guest/view_team.php?teams_id=17.

[59] M. Mathias, R. Makharia, H.A. Gasteiger, J.J. Conley, T.J. Fuller, C.J. Gittelman, S.S. Kocha, D.P. Miller, C.K. Mittelstead̈t, T. Xie, S.G. Yan, P.T. Yu, Interface 14 (2005) 24–35.

[60] M. Mathias, H. Gasteiger, R. Makharia, S. Kocha, T. Fuller, T. Xie, J. Pisco, Preprints – Am. Chem. Soc. Div. Fuel Chem. 49 (2004) 471–474.

[61] X. Wang, D. Myers, R. Kumar, Annual Progress Report, DOE Hydrogen Program, U.S. Department of Energy, Washington, DC, p. 920, 2006.

[62] S. Knights, 4th Annual Inter. Fuel Cell Testing Workshop, Vancouver, BC, Canada, September 12–13, 2007.

[63] J. Xie, D.L. Wood III, K.L. More, P. Atanassov, R.L. Borup, J. Electrochem. Soc. 152 (2005) A1011–A1020.

[64] H. Xu, R. Kunz, J.M. Fenton, Electrochem. Solid-State Lett. 10 (2007) B1–B5.

[65] S. Mitsushima, S. Kawahara, K. Ota, N. Kamiya, J. Electrochem. Soc. 154 (2007) B153–B158.

[66] R. Ornelas, A. Stassi, E. Modica, A.S. Aricò, V. Antonucci, ECS Trans. 3 (2006) 633–641.

[67] X.P. Wang, R. Kumar, D.J. Myers, Solid-State Lett. 9 (2006) A225–A227.

[68] W. Bi, T.F. Fuller, J. Electrochem. Soc. 155 (2008) B215–B221.

[69] W. Bi, G.E. Gray, T.F. Fuller, Electrochem. Solid-State Lett. 10 (2007) B101–B104.

[70] E. Guilminot, A. Corcella, F. Charlot, F. Maillard, M. Chatenet, J. Electrochem. Soc. 154 (2007) B96–B105.

[71] R.L. Borup, J.R. Davey, F.H. Garzon, D.L. Wood, M.A. Inbody, J. Power Sources 163 (2006) 76–81.

[72] Y.Y. Shao, G.P. Yin, Y.Z. Gao, P.F. Shi, J. Electrochem. Soc. 153 (2006) A1093–A1097.

[73] V.A.T. Dam, F.A. de Bruijn, J. Electrochem. Soc. 154 (2007) B494–B499.

[74] K.L. More, Microstructural characterization of PEM fuel cell MEAs, 2005 DOE H2 Program Review Proceedings, May 2005.

[75] J. Frisk, W. Boand, M. Hicks, M. Kurkowski, R. Atanasoski, A. Schmoeckel, 2004 Fuel Cell Seminar, San Antonio, TX, USA, November 1–5, 2004.

[76] R. Makharia, S.S. Kocha, P.T. Yu, M.A. Sweikart, W.B. Gu, F.T. Wagner, H.A. Gasteiger, ECS Trans. 1 (2006) 3–18.

[77] M. Crum, W. Liu, ECS Trans. 3 (2006) 541–550.

[78] A. Ohma, S. Suga, S. Yamamoto, K. Shinohara, J. Electrochem. Soc. 154 (2007) B757–B760.

[79] M.T. Hicks, 2006 Annual Progress Report, DOE Hydrogen Program, U.S. Department of Energy, Washington, DC, p. 722, 2006.

[80] D. Pierpont, M. Hicks, T. Watschke, P. Turner, ECS Trans. 1 (2006) 229–237.

[81] W. Liu, K. Ruth, G. Rusch, J. New Mater. Electrochem. Syst. 4 (2001) 227–232.

[82] C.A. Wilkie, J.R. Thomsen, M.L. Mittleman, J. Appl. Polym. Sci. 42 (1991) 901–909.

[83] S.R. Samms, S. Wasmus, R.F. Savinell, J. Electrochem. Soc. 143 (1996) 1498–1504.

[84] U. Beuscher, S.J.C. Cleghorn, W.B. Johnson, Int. J. Energy Res. 29 (2005) 1103–1112.

[85] J.R. Yu, T. Matsuura, Y. Yoshikawa, M.N. Islam, M. Hori, Electrochem. Solid-State Lett. 8 (2005) A156–A158.

[86] H.L. Tang, P.K. Shen, S.P. Jiang, F. Wang, M. Pan, J. Power Sources 170 (2007) 85–92.

[87] R.C. McDonald, C.K. Mittelsteadt, E.L. Thompson, Fuel cells 4 (2004) 208–213.

[88] E. Cho, J.-J. Ko, H.Y. Hong, S.-A. Hong, K.-Y. Lee, T.-W. Lim, I.-H. Oh, J. Electrochem. Soc. 51 (2004) A661–A665.

[89] X. Huang, R. Solasi, Y. Zou, M. Feshler, K. Reifsnider, D. Condit, S. Burlatsky, T. Madden, J. Polym. Sci. 16 (2006) 2346–2357.

[90] M. Inaba, T. Kinumoto, M. Kiriake, R. Umebayashi, A. Tasaka, Z. Ogumi, Electrochim. Acta 51 (2006) 5746–5753.

[91] S. Kundu, L.C. Simon, M.W. Fowler, Polym. Degrad. Stabil. 93 (2008) 214–224.

[92] S. Kim, B.K. Ahn, M.M. Mench, J. Power Sources 179 (2008) 140–146.

[93] R. Mukundan, Y.S. Kim, F. Garzon, B. Pivovar, ECS Trans. 1 (2006) 403–413.

[94] M. Oszcipok, D. Riemann, U. Kronenwett, M. Kreideweis, M. Zedda, J. Power Sources 145 (2005) 407–415.

[95] J. Frisk, W. Boand, M. Kurkowski, R. Atanasoski, A. Schmoeckel, 2004 Fuel Cell Seminar, San Antonio, TX, USA, November, 2004.

[96] D. Wood, J. Davey, F. Garzon, P. Atanassov, R.L. Borup, 2005 Fuel Cell Seminar, Palm Springs, CA, November, 2005.

[97] J. Martin, J. Wu, H. Wang, Ballard – NRC IFCI joint research project on gas diffusion layer accelerated stress testing, IFCI technical report, IFCI-PEMFC-CTR-046, January 2007.

[98] J. Martin, J. Wu, H. Wang, Ballard – NRC IFCI joint research project on gas diffusion layer accelerated stress testing, IFCI-PEMFC-CTR-055, June 2007.

[99] J. Martin, J. Wu, H. Wang, Ballard – NRC IFCI joint research project on gas diffusion layer accelerated stress testing, IFCI-PEMFC-CTR-066, October 2007.

[100] F-Y. Zhang, S.G. Advani, A.K. Prasad, M.E. Boggs, S.P. Sullivan, T.P. Beebe Jr., Electrochim. Acta 54 (2009) 4025–4030.

[101] J. Hou, W. Song, H. Yu, Y. Fu, L. Hao, Z. Shao, B. Yi, J. Power Sources 176 (2008) 118–121.

[102] F. Rong, C. Huang, Z.-S. Liu, D. Song, Q. Wang, J. Power Sources 175 (2008) 712–723.

[103] R. Borup, J. Davey, D. Wood, F. Garzon, M. Inbody, DOE Hydrogen Program, FY 2005 Progress Report 1039–1045.

[104] R. Borup, J.R. Davey, A.B. Ofstad, H. Xu, R. Mukundan, F. Garzon, B.S. Pivovar, 2008 Fuel Cell Seminar, LA-UR-08-4975.

[105] U.S. Department of Transportation, Final Report: Fuel Cell for Transportation Applications, FTA-IL-26-7006-2009.1, available at http://www.fta.dot.gov/documents/Fule_Cells_for_Transportation_Applications_FTA-IL-26-7006-2009.1.pdf.

[106] FCTestNet. 2006. WP2 Stationary Fuel Cell Systems: Test Programs and Test Modules, available at http://fctesqa.jrc.ec.europa.eu/downloads/Stationary/060603%20FCTESTNET%20Stationary%20Applications.pdf.

[107] JRC scientific and technical reports, Testing the voltage and the power as a function of the current density following an on/off profile versus time (accelerated ageing on/off cycling test for a PEFC single cell), Test Module PEFC SC 5-4, 2010, available at http://fctesqa.jrc.ec.europa.eu/downloads/PEMSCLV/OnOff_ageing_cycle_TestProcedure.pdf.